Characterization and Modeling of InP-based Single Photon Avalanche Diodes for 1.5 µm and 1.06 µm Photon Counting

Mark Itzler

Princeton Lightwave Inc., Cranbury, NJ USA

Co-authors and Collaborators

<u>**PLI CO-AUTHORS:**</u> **Xudong Jiang, Rafael Ben-Michael, Krystyna Slomkowski**

<u>**COLLABORATORS for device characterization:**</u>
Bruce Nyman......*PLI*
Mark Entwistle

Sergio Cova........*Politecnico di Milano*
Alberto Tosi
Franco Zappa

Mike Krainak.......*NASA/GSFC*
Stewart Wu
Xiaoli Sun

Radu Ispasoiu.....*Credence Systems*

Gary Smith..........*MIT Lincoln Laboratories*

Gerald Buller......*Heriot-Watt University*
Sara Pelligrini

Motivation for single photon detectors

Princeton Lightwave

Examples of photon counting applications for λ > 1.0 – 1.6 μm:

- **Communications**
  - Secure communications (e.g., quantum key distribution)
  - Free space optical communication in photon-starved applications
- **Remote sensing**
  - 3-D Imaging
  - Lidar / atmospheric sensing
- **Industrial and Biomedical**
  - Semiconductor diagnostics
  - Single photon fluorescence (e.g., quantum dot markers)

Presentation outline

- Overview of InP-based single photon avalanche diodes (SPADs)
- Dark count rate vs. detection efficiency
- Afterpulsing effects (and impact on photon counting rate)

InGaAsP/InP avalanche diode design platform

- **Separate Absorption, Charge, and Multiplication (SACM) structure**
  - High E-field in multiplication region → induce avalanching
  - Low E-field in absorption region → suppress tunneling
- **Planar passivated, dopant diffused device structure**
  - Stable and reliable buried p-n junction
  - Widespread deployment of device platform in telecom Rx

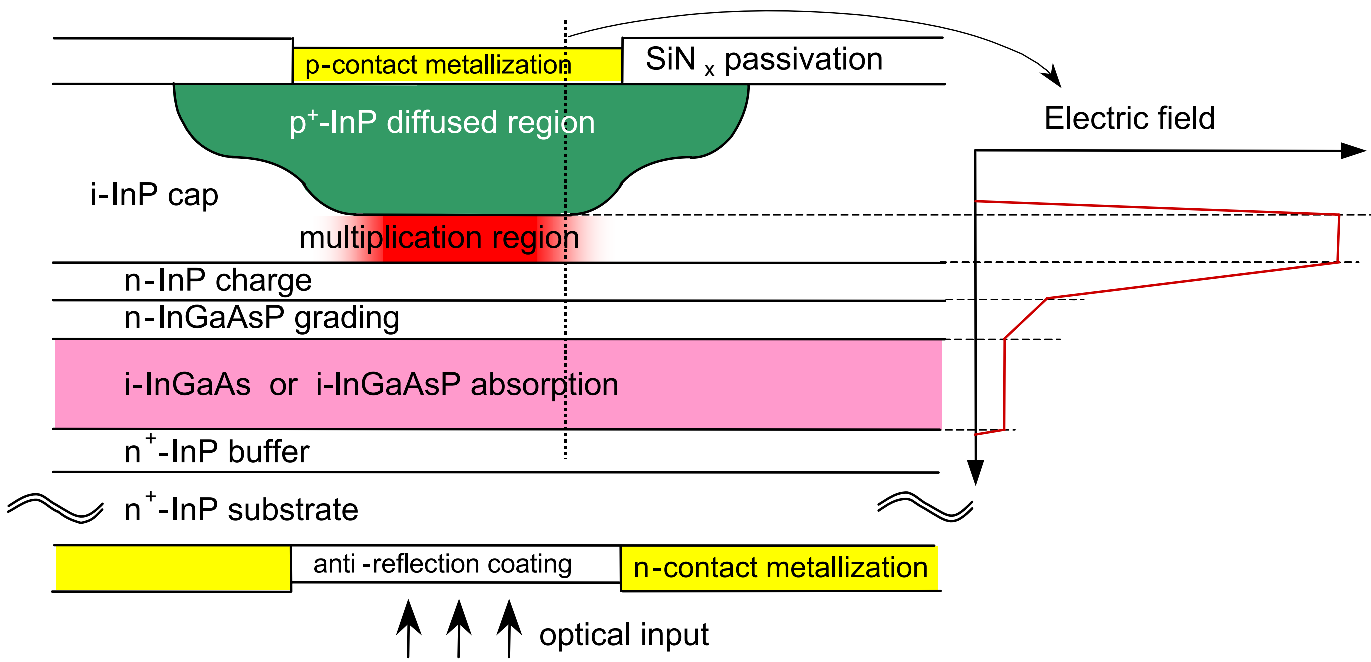

APD Current-Voltage Characteristics

- Linear mode performance is behavior below breakdown voltage V_b
  - Output photocurrent below V_b is linearly proportional to input optical power

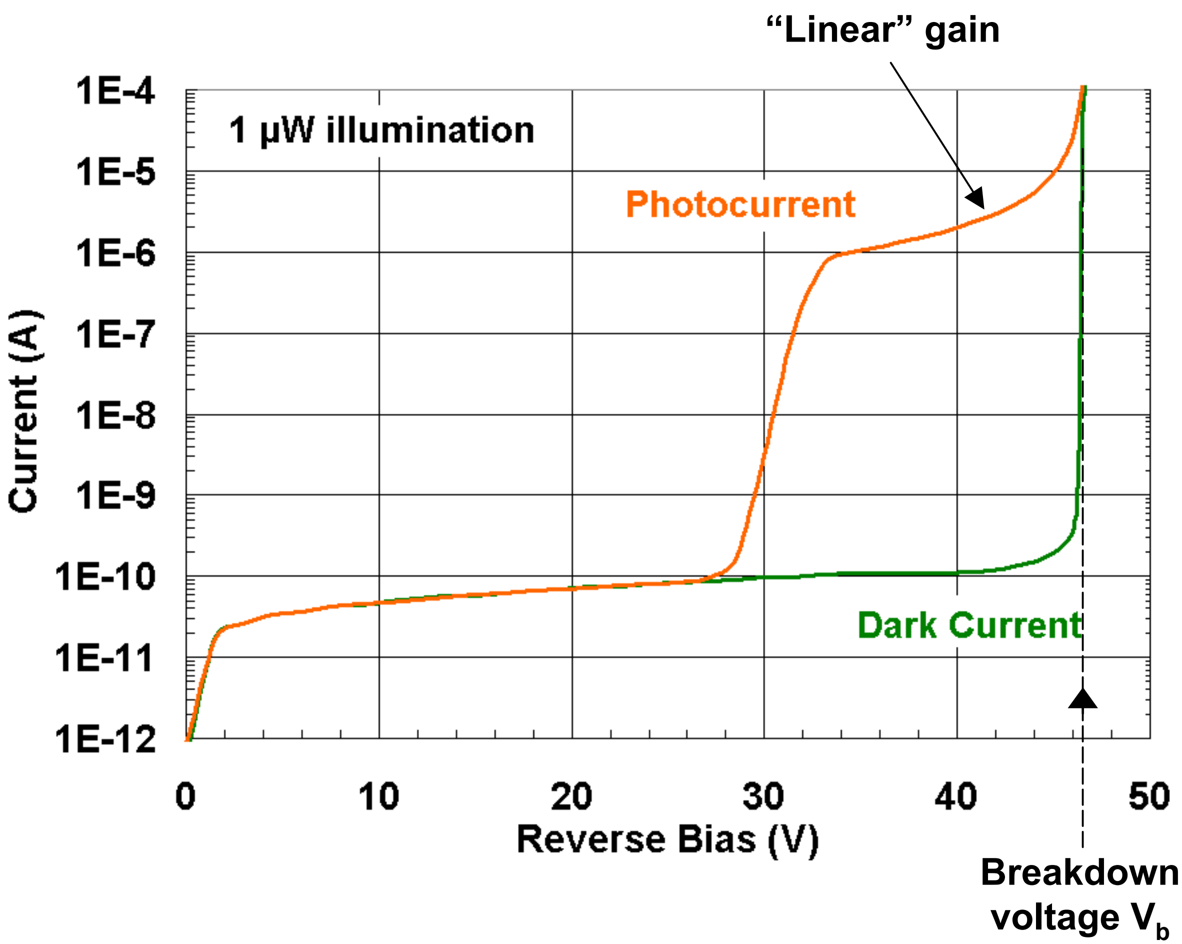

Performance uniformity at wafer level

- Breakdown voltage is very sensitive to structural details
  - Provides good measure for consistency of many device attributes

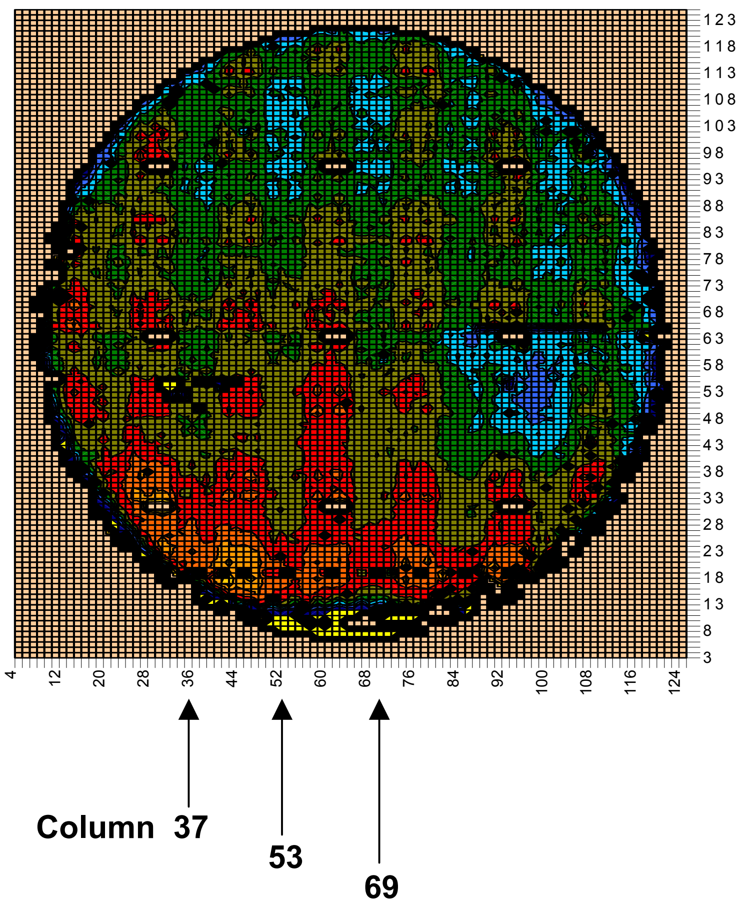

- Ex.: 1.06 μm SPAD wafer
- Intentional systematic variation to confirm diffusion control process
- **V_b variation: ~ 0.03 V per mm**

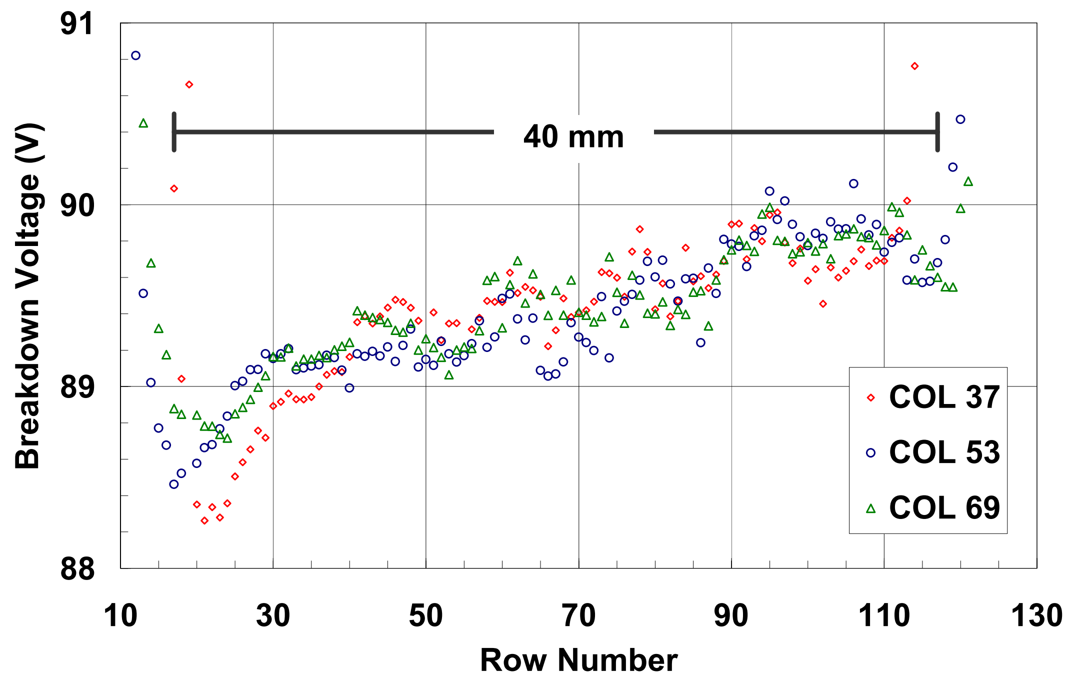

Geiger mode operation

- **Single photon avalanche diodes (SPADs) operate in "Geiger mode"**
  - Bias above breakdown voltage V_b by overbias ΔV
  - Single photon induces avalanche leading to macroscopic current pulse
    - Avalanche detected using threshold detection circuit
  - Used as a photon-activated switch with purely digital output
  - Avalanche must be quenched after detection by lowering bias below V_b

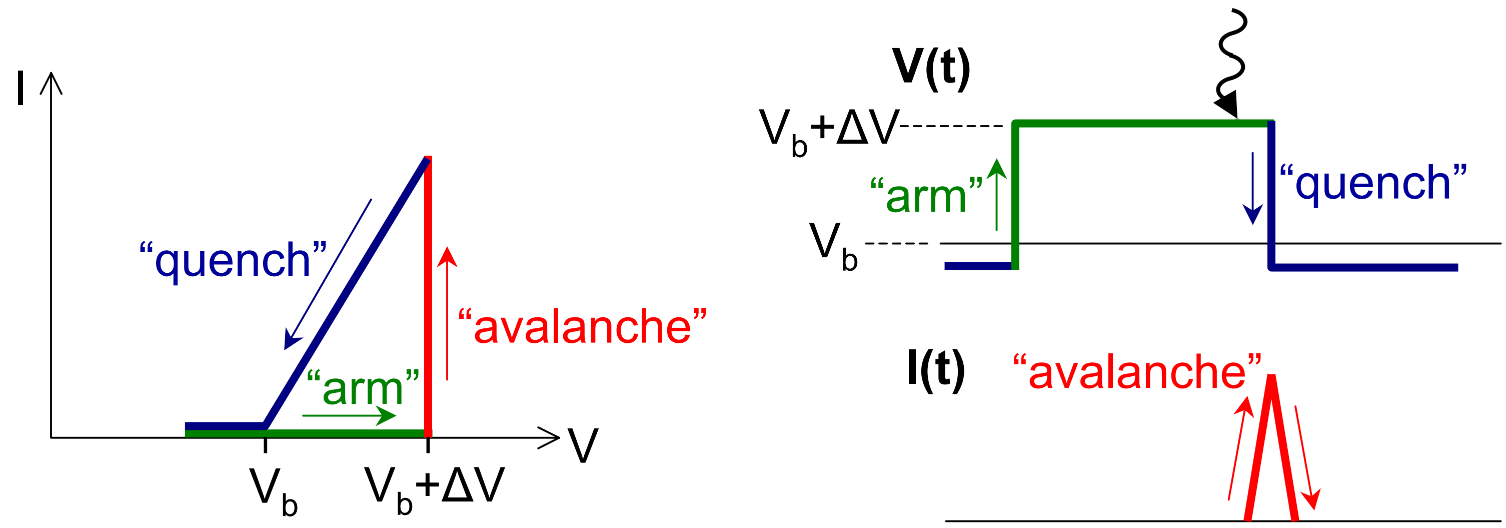

Presentation outline

- Overview of InP-based single photon avalanche diodes (SPADs)
- **Dark count rate vs. detection efficiency**
- Afterpulsing effects (and impact on photon counting rate)

DCR vs. DE trade-off

- **Most important SPAD performance tradeoff: DCR vs. DE**
- Typical performance: 10 kHz DCR at 20% DE, 100 kHz at 40% DE

Data for 25 μm diameter InGaAs/InP SPADs for 1.5 μm

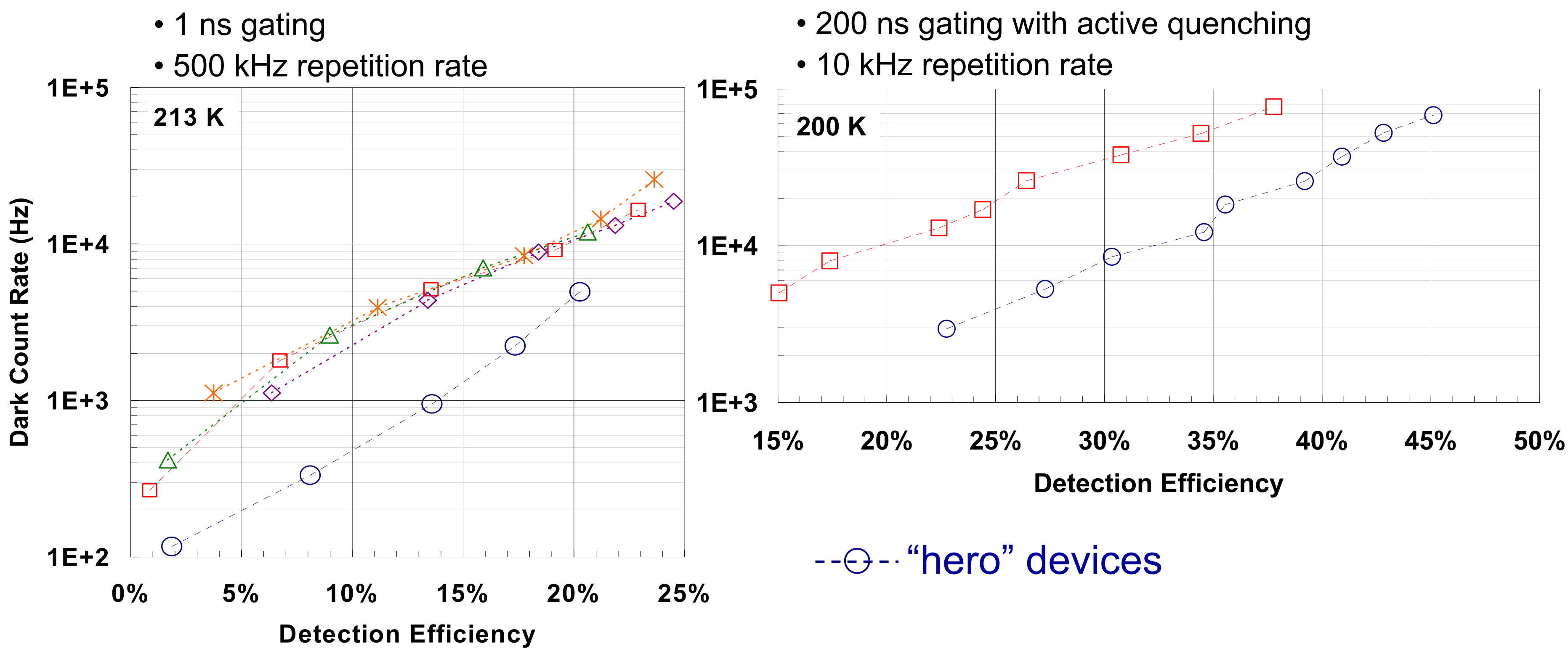

Dark count rate behavior and mechanisms

- Simulations give insight into dominant DCR mechanisms
  - following formalism of Donnelly *et al.* [JQE 42, p. 797 (2006)]
- Dark carriers can be generated by a number of mechanisms

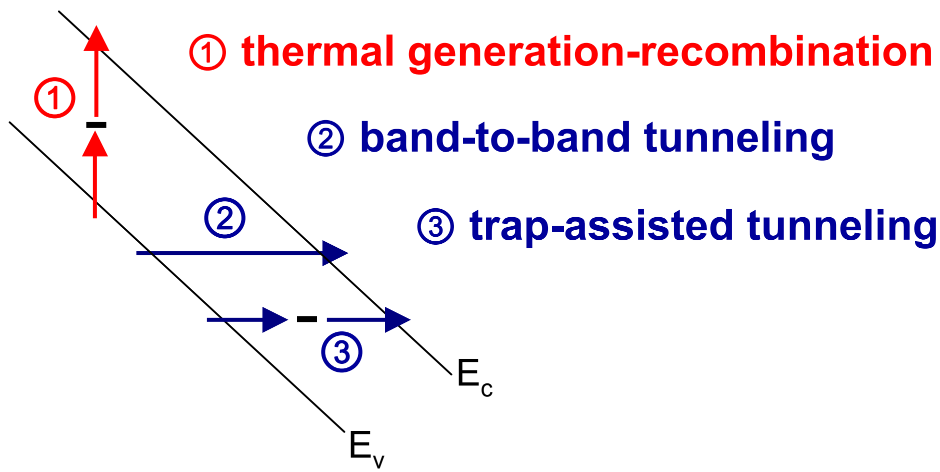

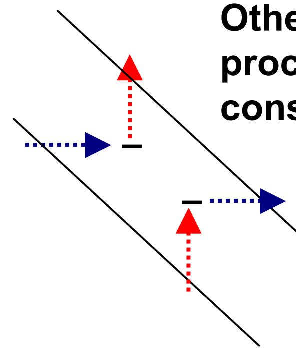

Other “combined” processes not considered

- Sample properties will have a large impact on DCR
  - Bandgap (InP vs. InGaAs vs. InGaAsP)
  - Defects
- Study DCR dependence on temperature and voltage bias for clues
  - **Extract activation energies** to help identify dominant DCR mechanisms

DCR vs DE modeling for 1.5 μm SPADs

- Modeling provides reasonable fit to DCR vs DE behavior

- gated-mode operation
- 1 ns gate width
- 500 kHz repetition rate

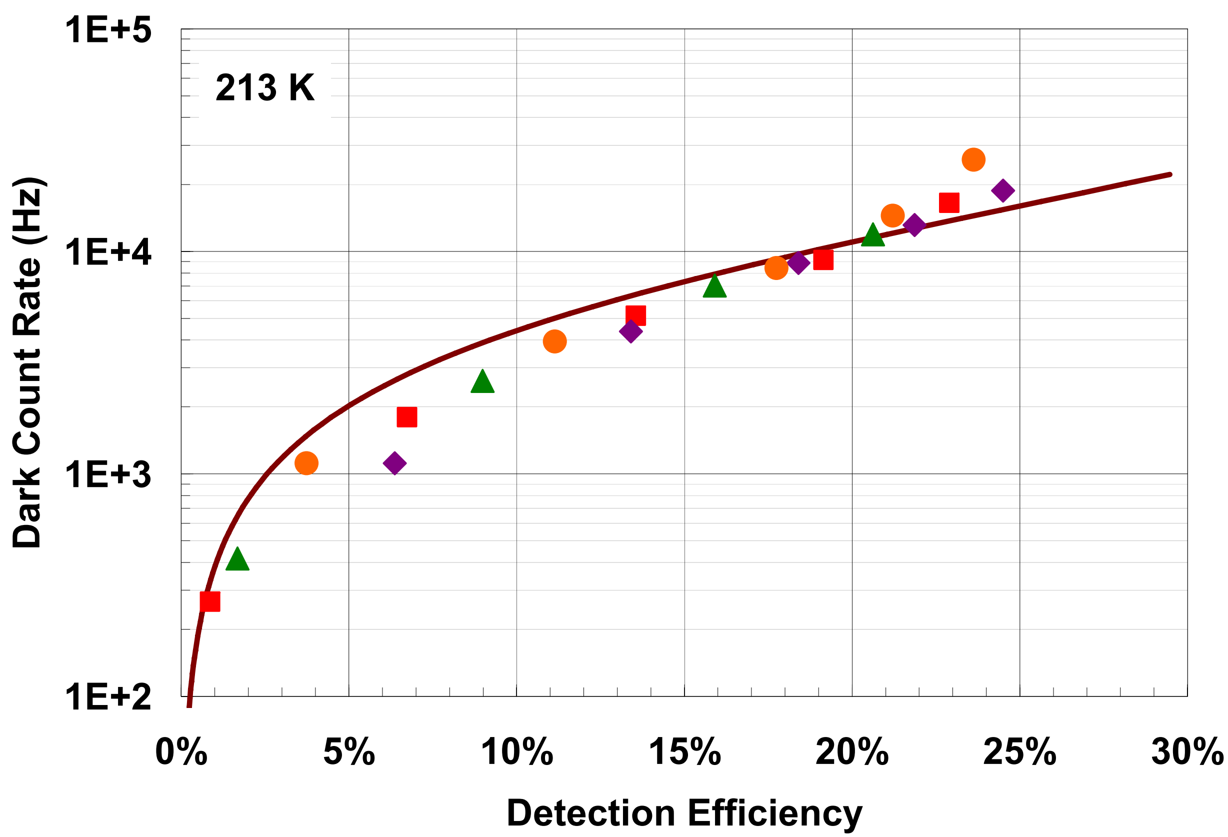

Dominant DCR mechanisms from modeling

- **Two dominant DCR mechanisms for 1.5 µm SPADs at 213 K**
  - Trap-assisted tunneling (TAT) in InP multiplication region
  - Thermal generation-recombination (G-R) in InGaAs absorber
- **TAT and G-R compete at low overbias (e.g., V_{ov} < 3 V)**

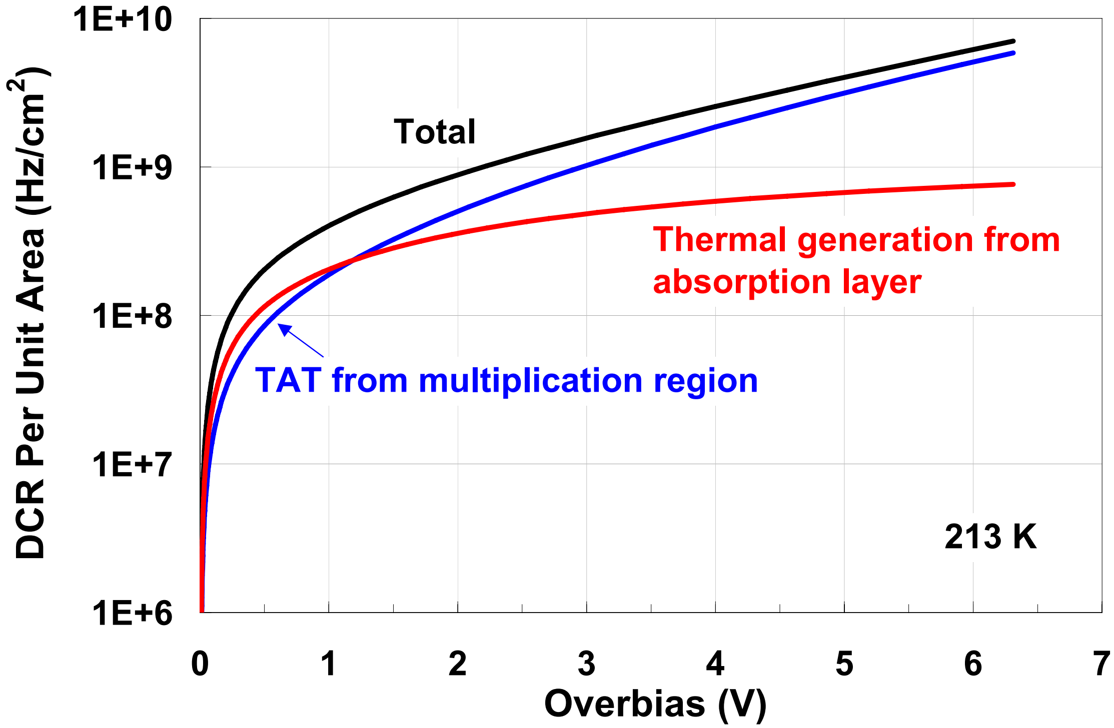

- **At higher temperatures, G-R dominates**

DCR vs. DE trade-off in 1.06 µm SPADs

- **Use InGaAsP absorber in structure similar to 1.5 µm SPADs**
  - Thermal G-R significantly reduced with wider bandgap InGaAsP
- **DCR approaching Si SPAD DCR with greatly increased PDE**
  - Si SPADs have PDE < 2% at 1.06 µm

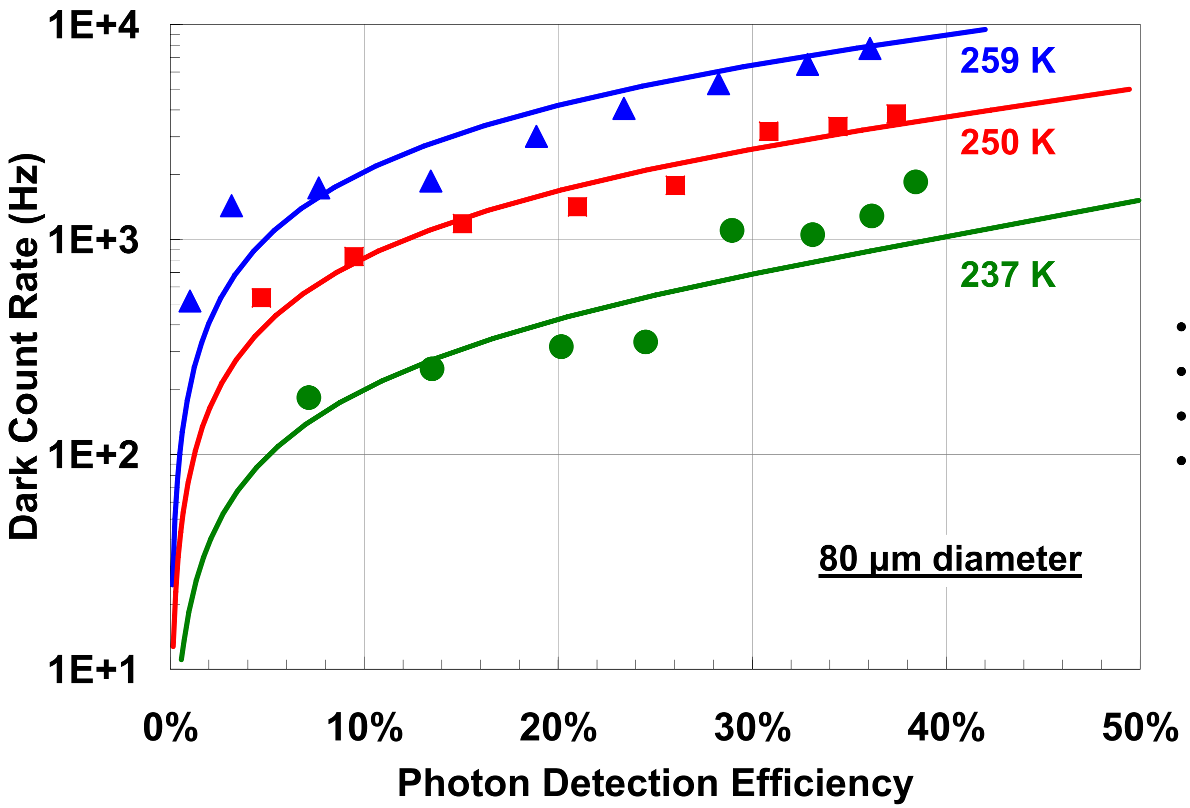

- **1.06 µm SPAD**
- **gated-mode operation**
- **1 ns gate width**
- **500 kHz repetition rate**

DCR mechanisms for 1.06 µm SPADs

- At low temp, multiplication region trap-assisted tunneling dominates
  - Thermal generation in absorber is inconsequential due to larger InGaAsP bandgap
- At room temp, two mechanisms compete
  - Similar to 1.5 µm SPADs at low temp (213 K)

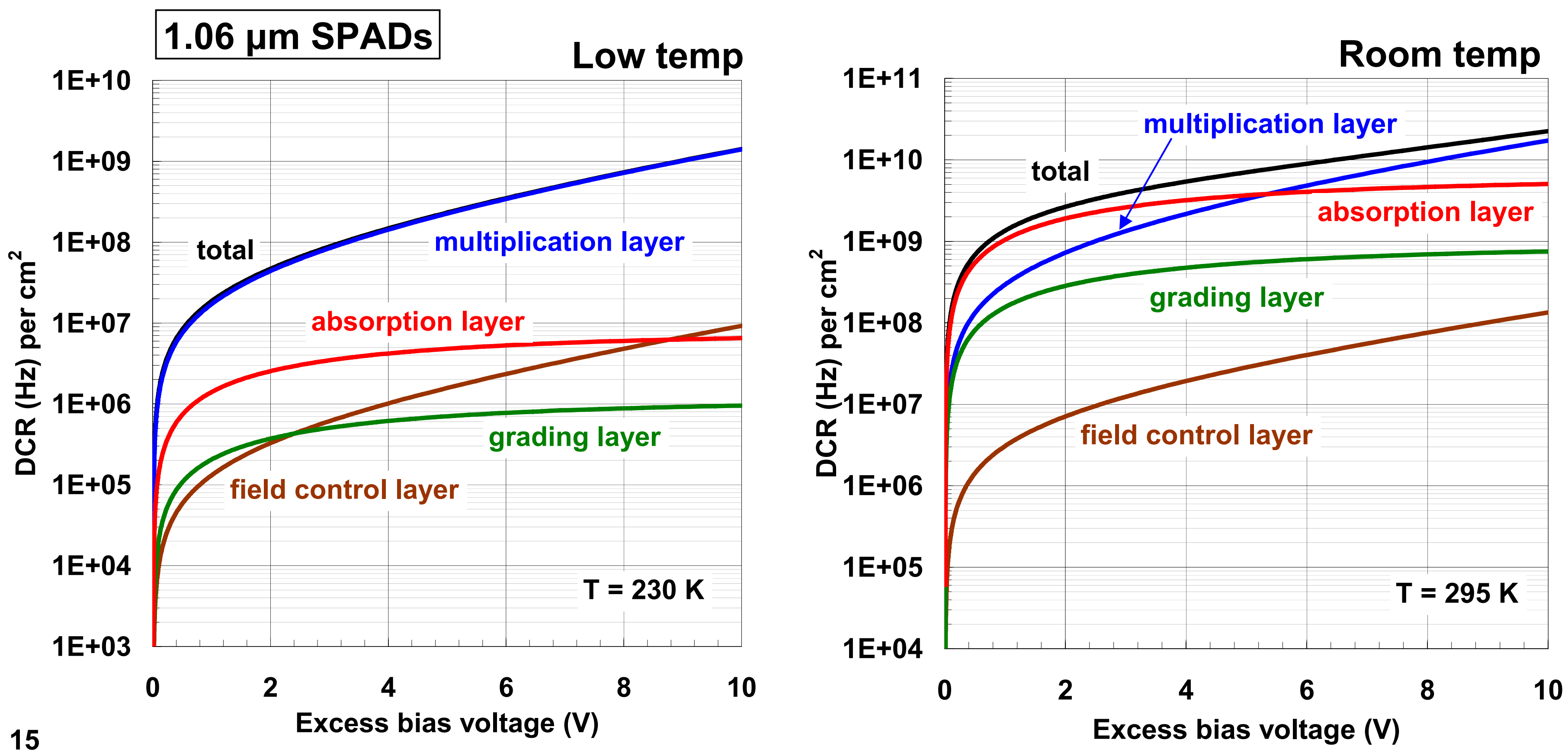

Confirm DCR mechanisms by studying E_a

- Characterize DCR vs. temperature at different overbias for T < 220 K
  - Assume DCR ~ $\exp(-E_a/kT)$ to extract activation energy E_a

1.5 µm SPAD

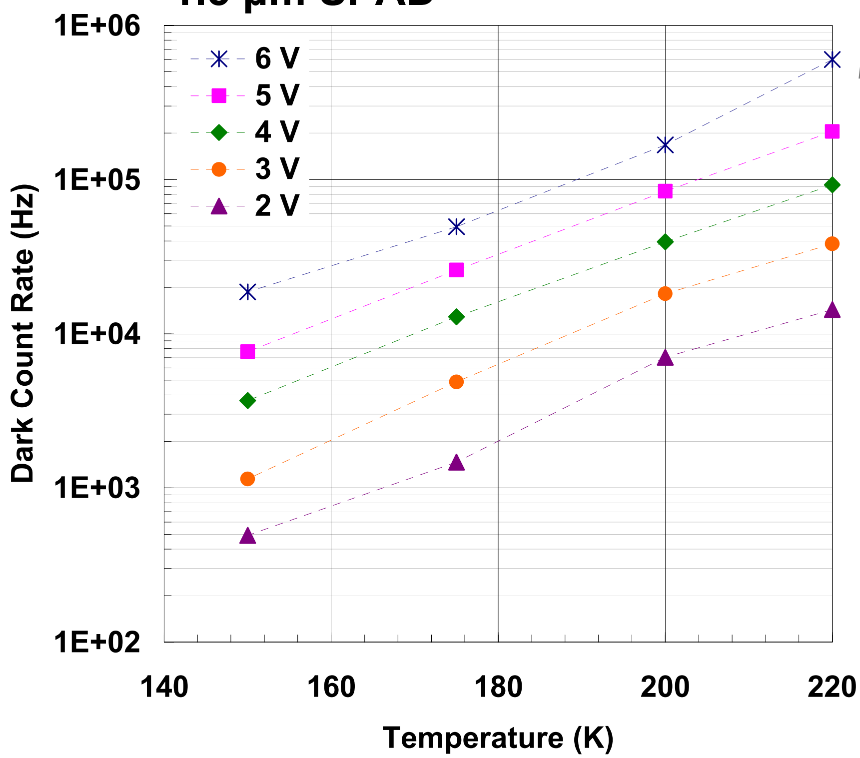

Plot DCR vs $(kT)^{-1}$

$\langle E_a \rangle$ ~ 0.14 eV

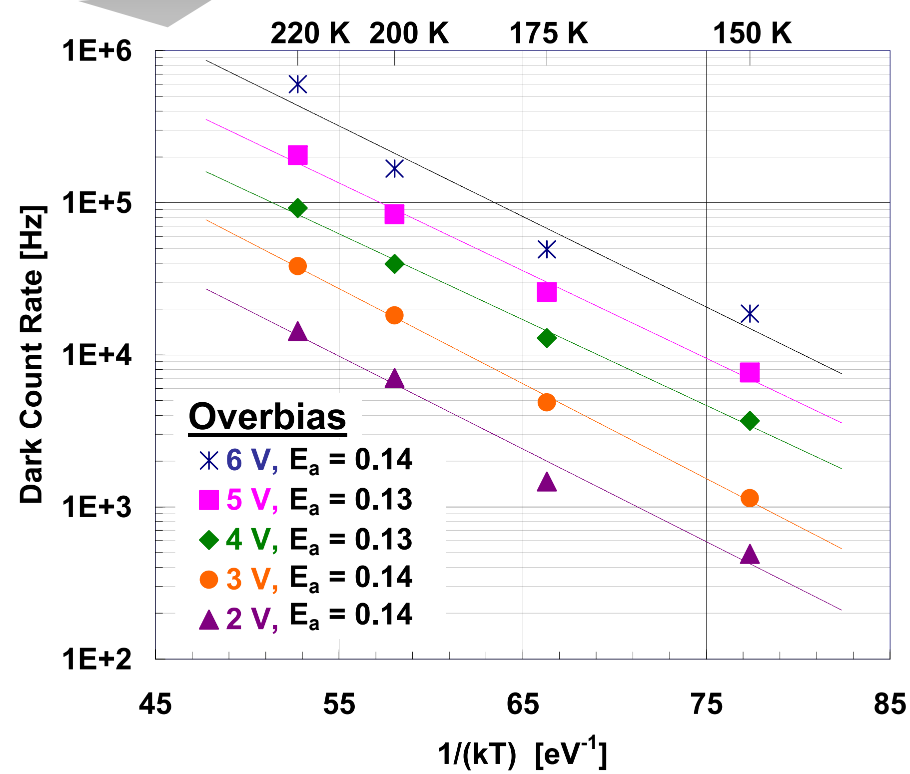

Itzler *et al*., J. Mod. Opt. 54, p 283 (2007)

Dark count rate behavior and mechanisms

- **DCR vs. temperature at different overbias for T > 200 K**
  - Can not fit with fixed E_a for T $\gtrsim$ 220 K

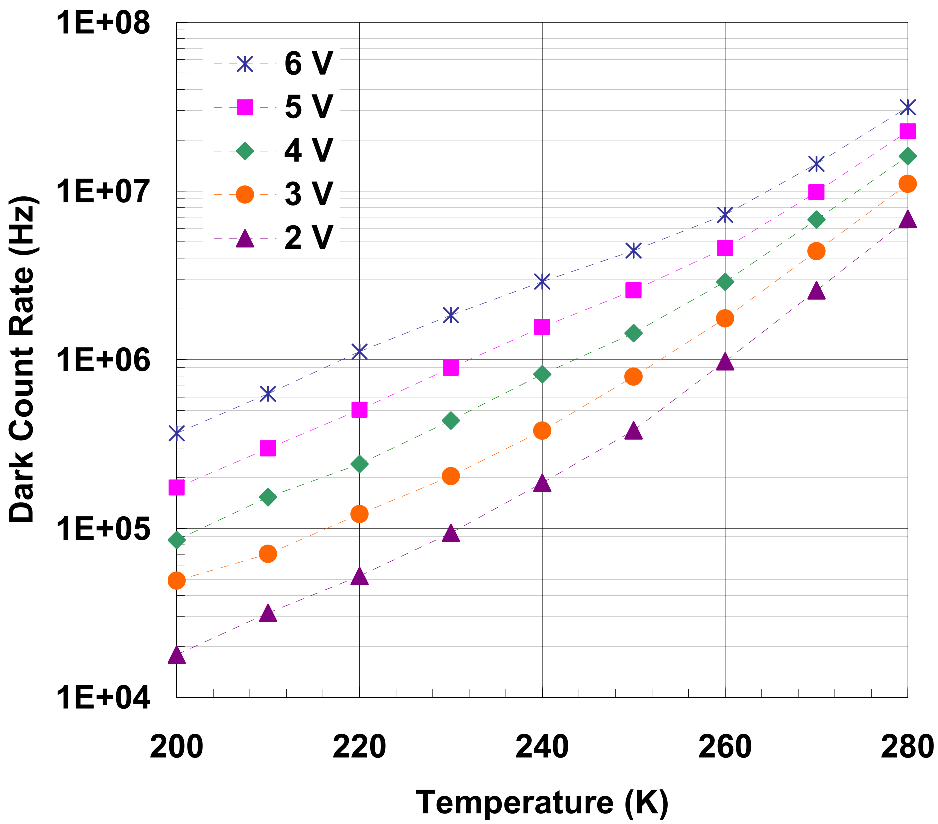

Characterization data from G. Smith, MIT/LL

Need to consider E_a(T):
change in E_a → change in dark carrier generation mechanism

Dark count rate behavior and mechanisms

- Consider T dependence of DCR activation energy $E_a(T)$
- Variation of Ea with T is consistent with DCR modeling results

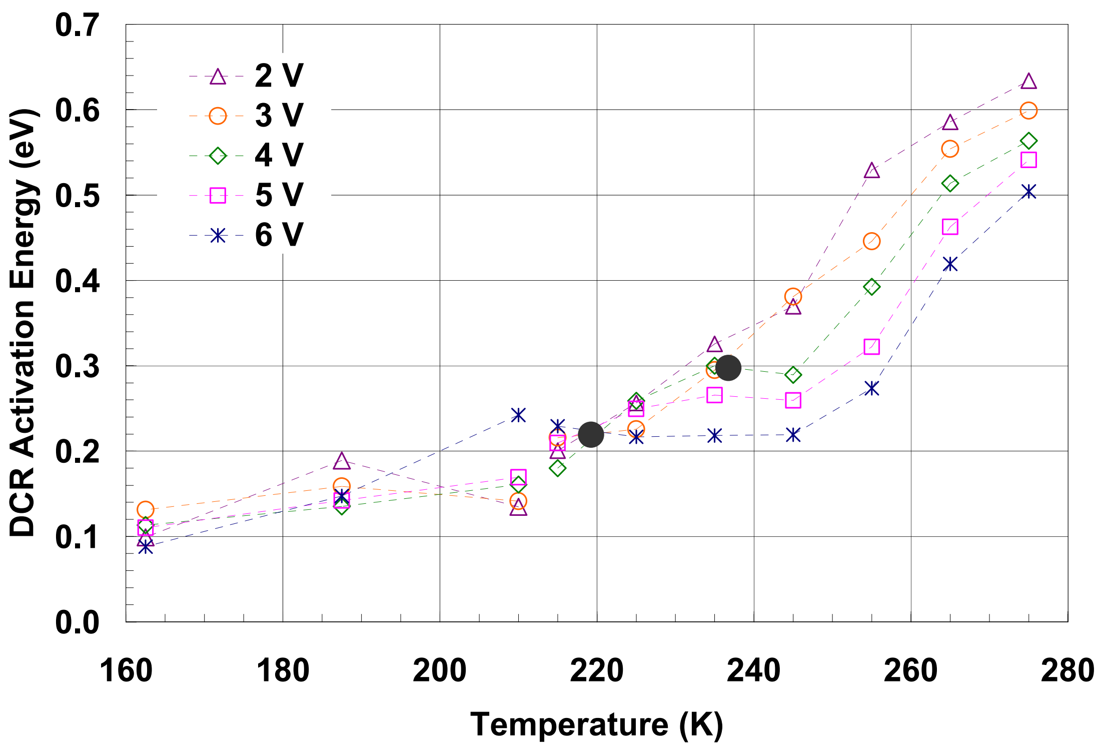

Open symbols, $T \lesssim 210$ K: 20 ns gating

Open symbols, $T \gtrsim 215$ K: 100 ns gating

"●" : 1 ns gating, ~3 V

- For $T \lesssim 230$, low $E_{a,\,DCR}$ → tunneling mechanisms
- For $T \gtrsim 230$, increasing $E_{a,\,DCR}$ → thermal generation becomes important
  - thermal generation more significant at low overbias

TAT defects in DCR modeling

- **G-R can be reduced by lower temperature operation**
- **TAT contribution is more fundamental**
  - Very sensitive to defect location in InP bandgap
  - Linear dependence on defect concentration
- **Modeling for 1.55 and 1.06 µm used same TAT defect location of 0.78E_g**
  - Good consistency with MIT/LL modeling results for 1.06 µm (0.75E_g)
  - Some consistency with highly varied older literature on native defects in InP
    - Possible origin with P vacancies in InP lattice [Verghese et al., JSTQE 13, 870 (2007)]

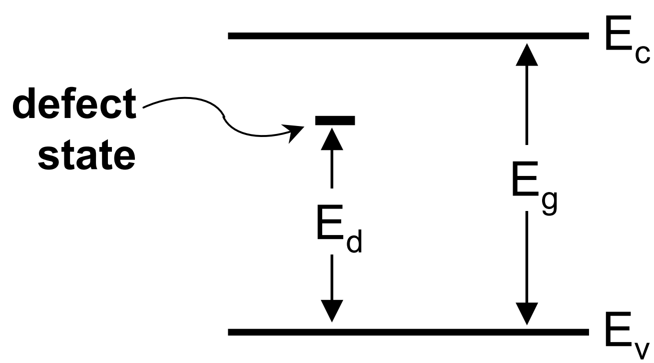

- Simulations very sensitive to defect attributes
- Need appropriate materials analysis (e.g., DLTS/capacitive spectroscopy)

Presentation outline

- Overview of InP-based single photon avalanche diodes (SPADs)
- Dark count rate vs. detection efficiency
- **Afterpulsing effects (and impact on photon counting rate)**

Description of afterpulsing

- **Afterpulsing is most serious limitation of InP SPADs; limits repetition rate**
- Avalanche carriers temporarily trapped at defects in InP multiplication region
- Carrier de-trapping at later times can initiate “afterpulse” avalanches
  - Afterpulsing likely if “hold-off” times $T_{h\text{-}o} \lesssim$ detrapping time τ_d

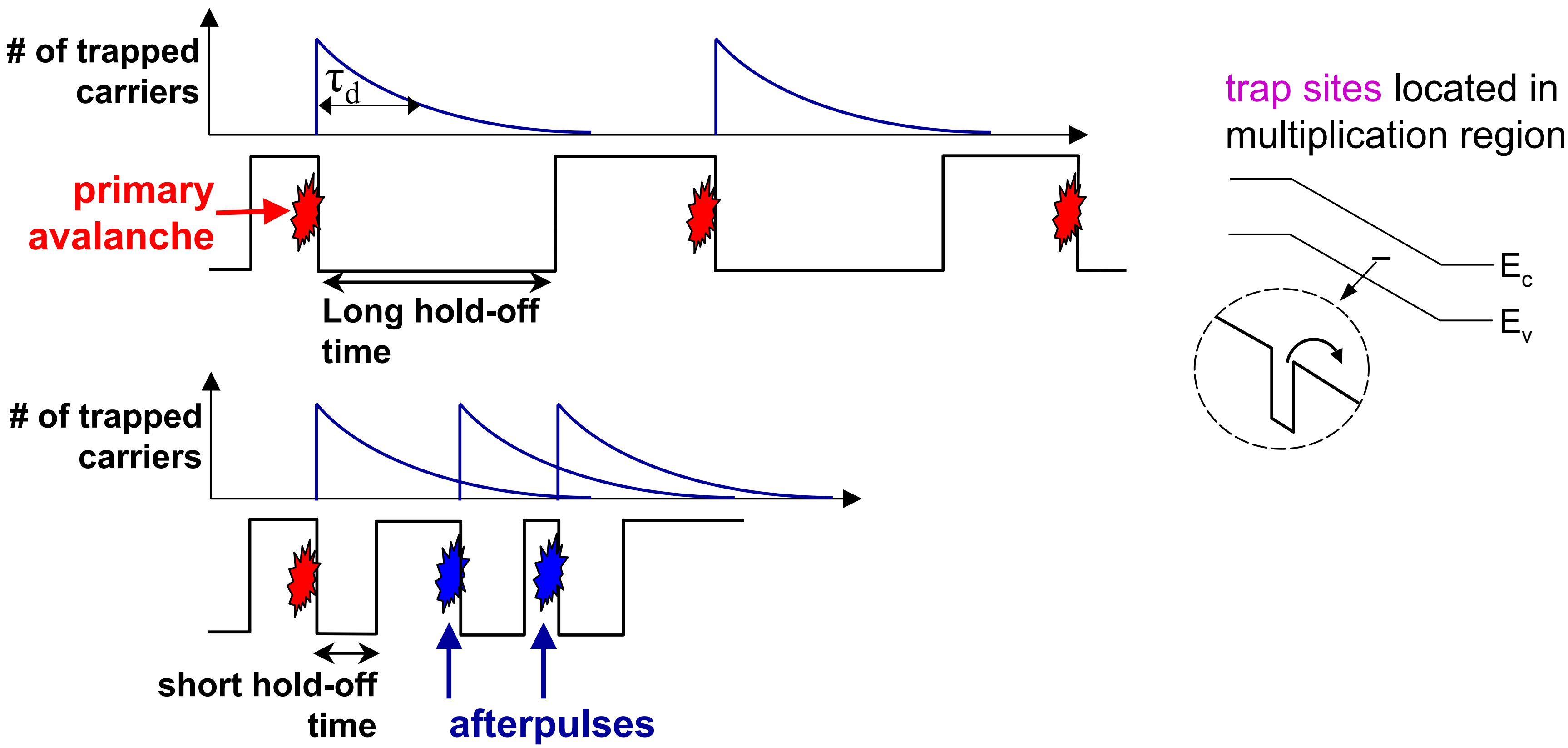

Afterpulse probability: short gate measurement

- **Assess afterpulsing using short (1 ns) gates as function of repetition rate**
  - Repetition rate varied from 0.5 MHz to 10 MHz
  - Photon arrival staggered to coincide with only “odd” gate pulses
  - Afterpulsing indicated by increased dark count rates in “even” pulses
- **5 MHz repetition rate maintains acceptable afterpulse probability**

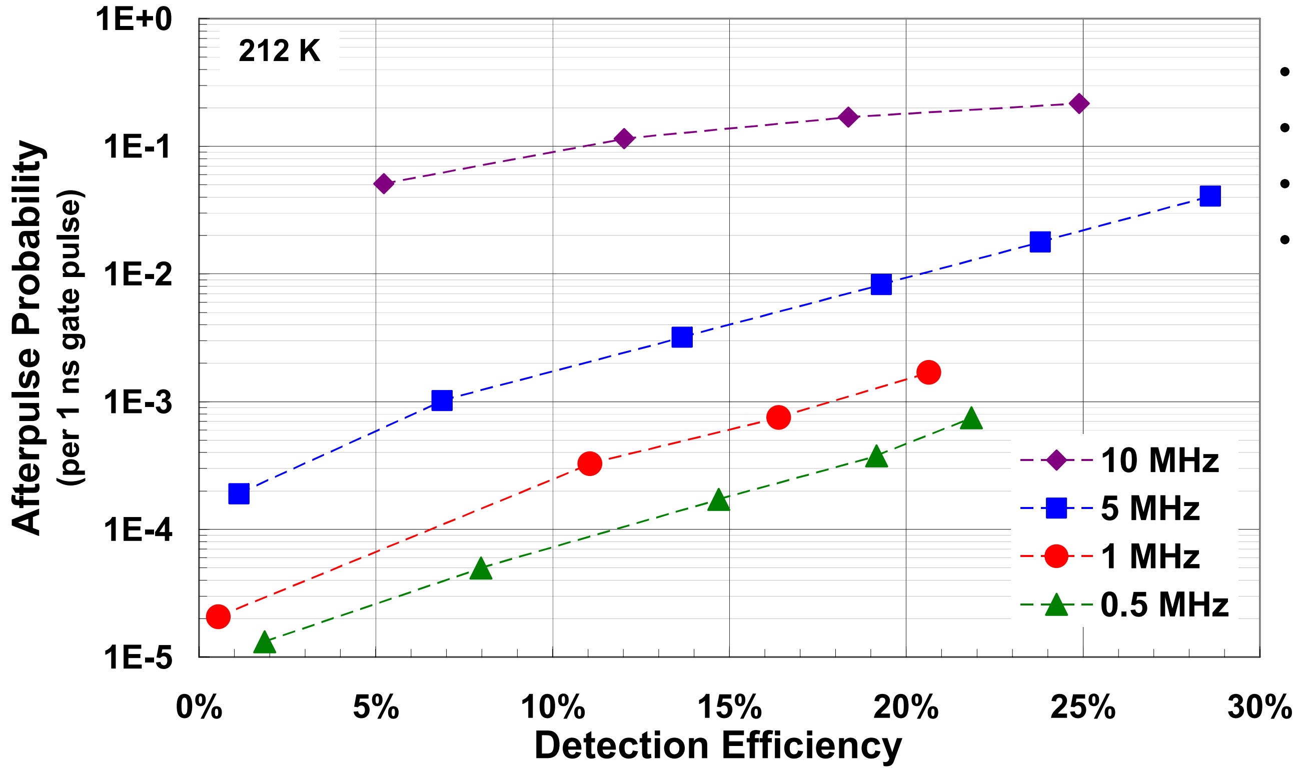

- **40 µm dia. SPADs**
- **gated operation**
- **1 ns gates**
- **212 K**

Impact of afterpulsing on dark count rates

- **Assess impact of afterpulsing through DCR dependence on hold-off time**
  - Looking at afterpulses induced by dark counts only
  - Sharp rise in DCR at short $T_{h\text{-}o}$ due to afterpulsing

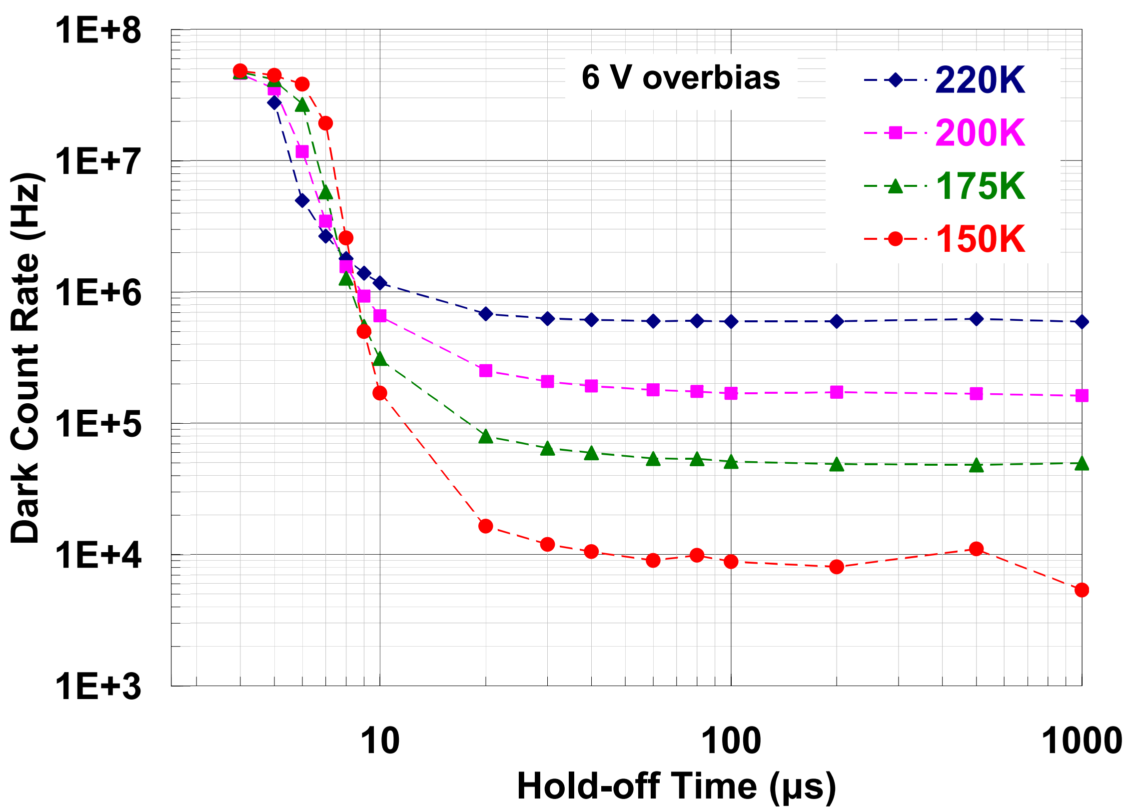

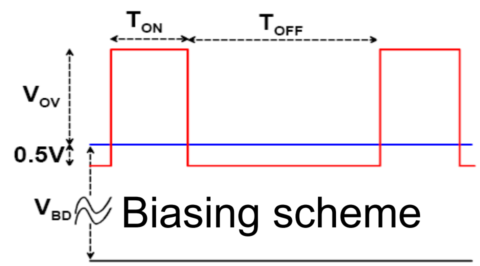

- **40 μm diameter SPADs**
- **20 ns gated quenching**
- **6 V overbias**

Characterization data from A. Tosi, S. Cova, F. Zappa

Temperature dependence of afterpulsing

- Normalize to background DCR → shows modest effect of temperature
- DCR vs. $T_{h\text{-}o}$ curves collapse to a single curve with correct rescaling
  - Same curve shape up to temperature-dependent scale factor for $T_{h\text{-}o}$

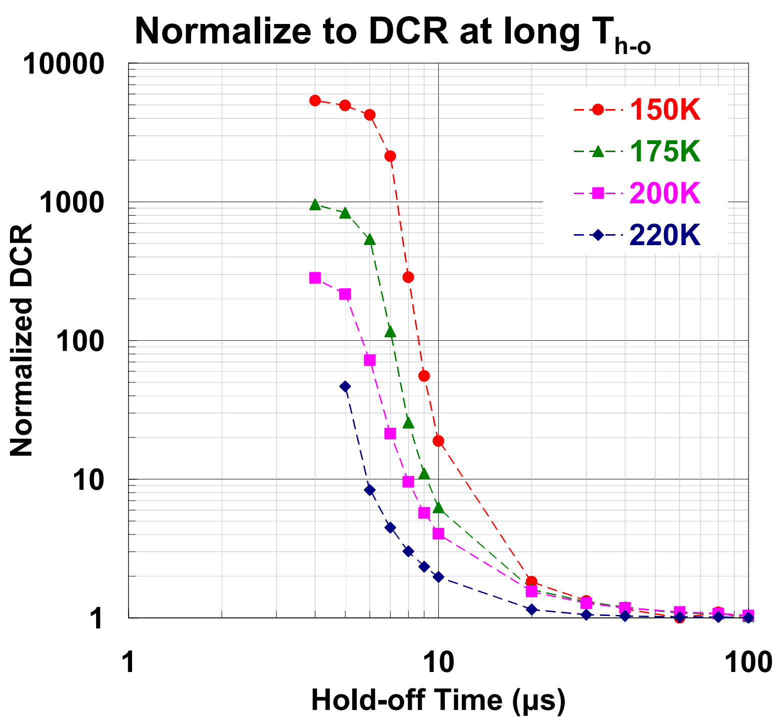

Scale factors

150 K: 1

175 K: 1.25

200 K: 1.45

220 K: 1.90

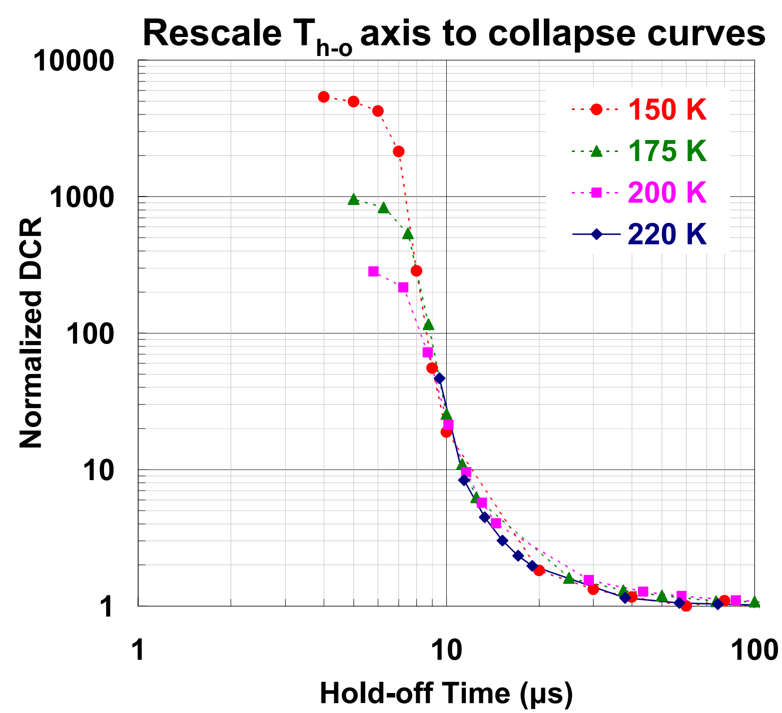

Xiang *et al*., JSTQE 13, 895 (2007)

Collapse allows extraction of afterpulsing activation energy

Afterpulsing activation energy $E_{a,AP}$

- Use DCR vs $T_{h\text{-}o}$ curve collapse to find afterpulse activation energy
  - Assuming single detrapping time τ_d , inverse of scale factor $\propto \tau_d$

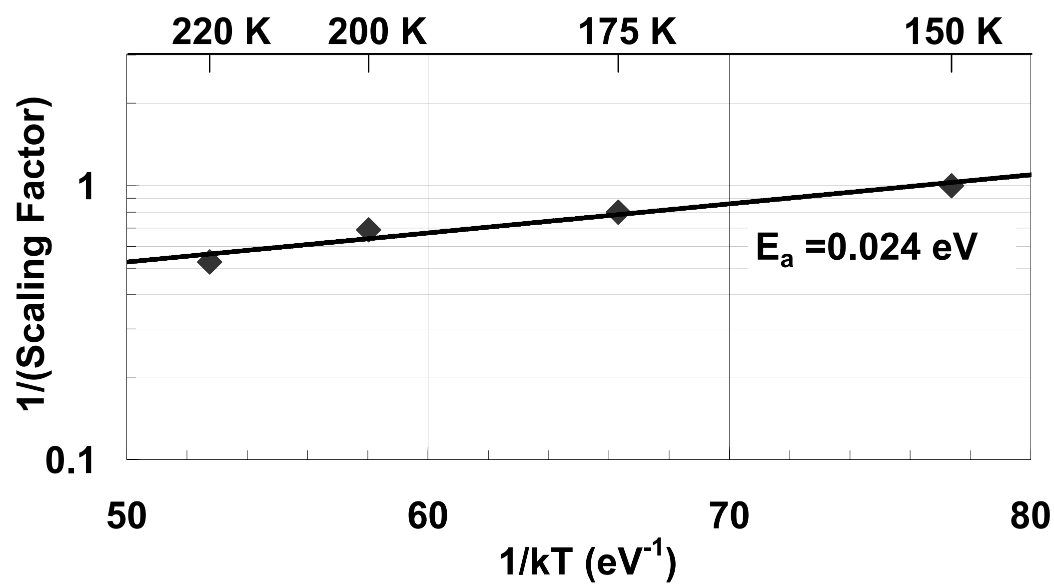

Scale factors

150 K: 1

175 K: 1.25

200 K: 1.45

220 K: 1.90

- Small $E_{a,AP}$ ~ 0.024 eV → change in AP between 150 K and 220 K is only 2X
- $E_{a,AP}$ increases at higher T, but still modest impact
  - change in AP between 220 K and 250 K is ~2X - 3X
- **Increased temperature does not provide much leverage for reducing AP**

Impact of gate length on afterpulsing

- Assess afterpulsing vs gate length using DCR vs $T_{h\text{-}o}$ data
- Simulation provides qualitative agreement with measured data
  - Assumes single detrapping time τ_d **following Kang et al.** [APL 83, 2955 (2003)]

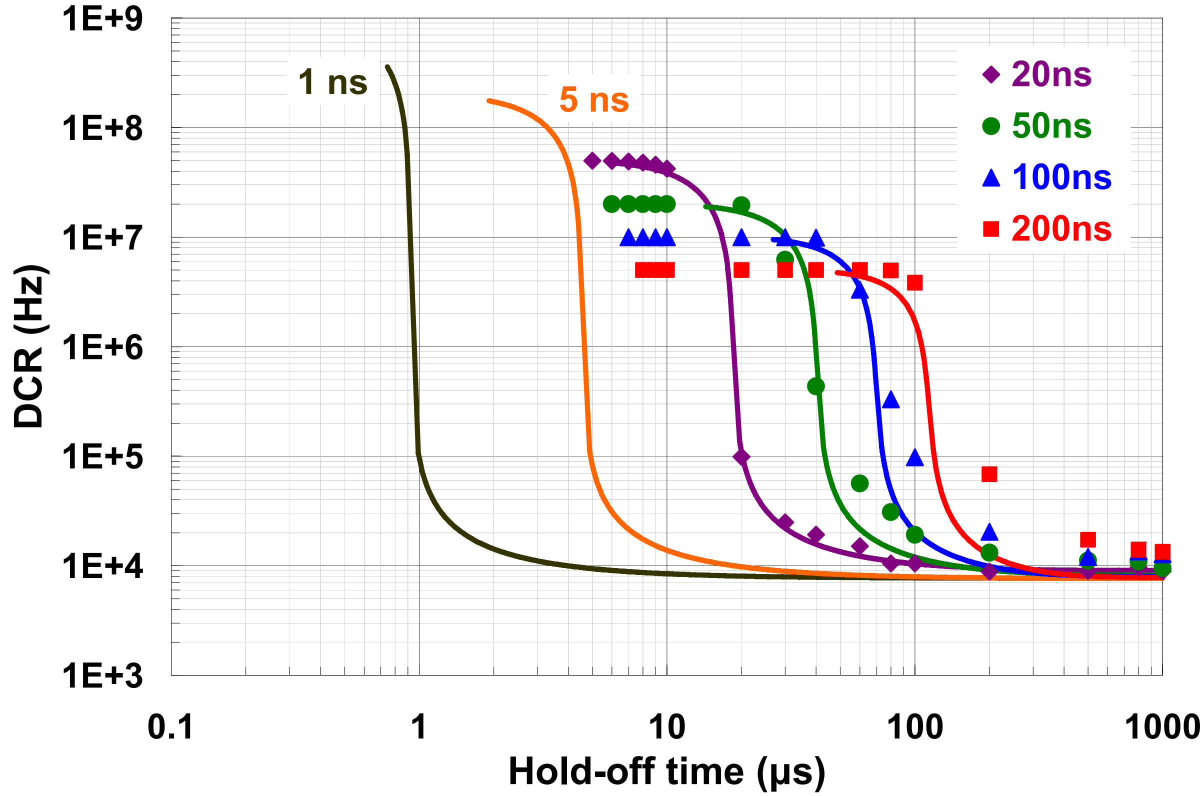

Points:
Measured

Solid lines:
Simulated

T = 150 K

Characterization data from A. Tosi, S. Cova, F. Zappa

- **Smaller current flow at shorter gates → greatly reduced afterpulsing**

Impact of overbias on afterpulsing

- **Low overbias reduces afterpulsing relative to high overbias**
  - 6 V overbias: very large DCR increase (> 100X) at $T_{h\text{-}o}$ = 4 μs
  - 2 V overbias: very small DCR increase (~ 2X) at $T_{h\text{-}o}$ = 4 μs

6 V overbias: high charge flow

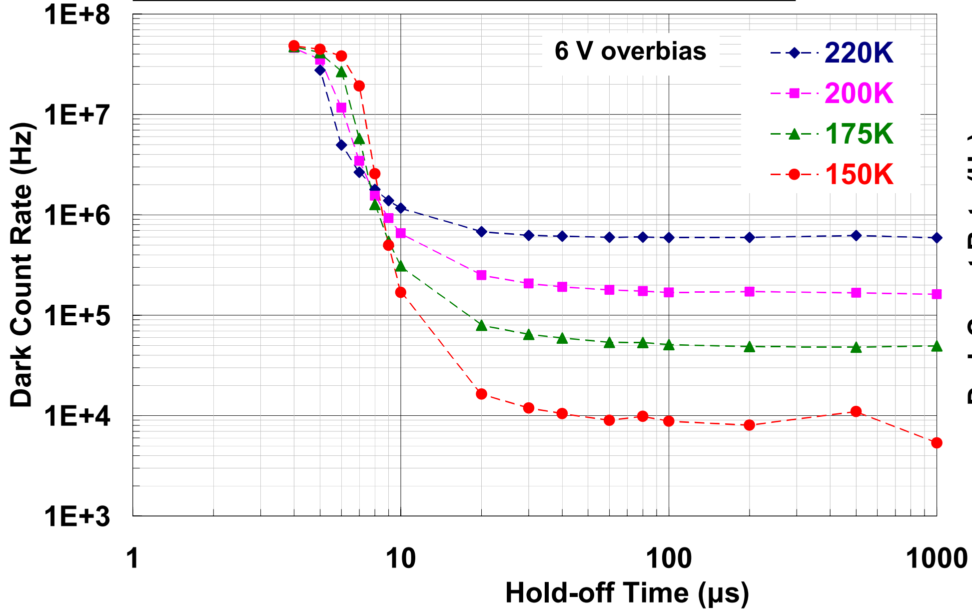

2 V overbias: low charge flow

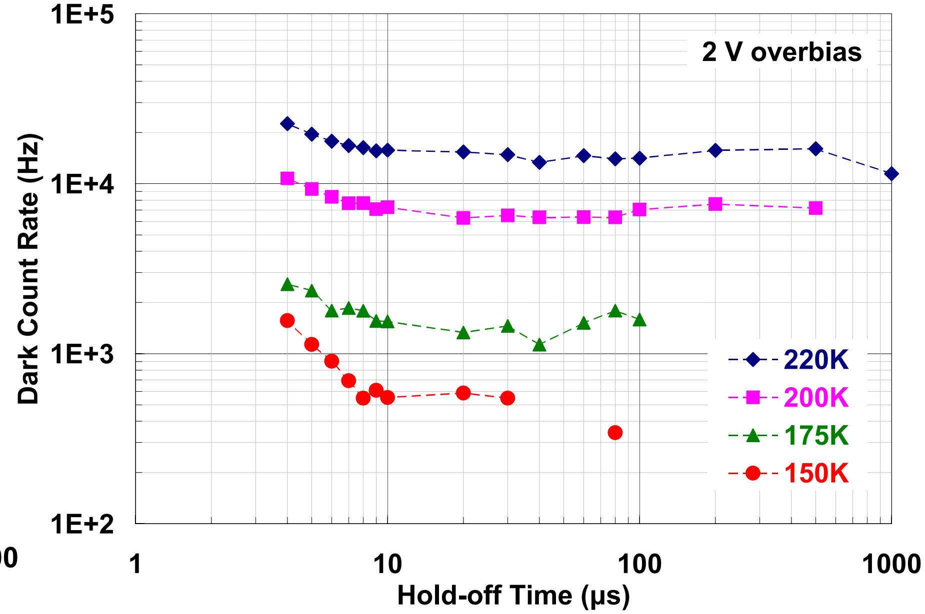

- **Smaller current flow at <u>lower overbias</u> → reduced afterpulsing**

Other issues related to afterpulsing

- **Single trap vs. multiple traps: fundamental question for modeling**
  - Multiple traps: too many free parameters, or correct physics?
- **De-trapping times found will depend on hold-off times $T_{h\text{-}o}$ used**
  - For narrow range of $T_{h\text{-}o}$, see just one de-trapping time from $R_{AP}(t)$

$$R_{AP}(t) = \frac{N_1}{\tau_1} e^{-t/\tau_1} + \frac{N_2}{\tau_2} e^{-t/\tau_2} + \frac{N_3}{\tau_3} e^{-t/\tau_3} + \ldots$$

Hypothetical multiple-trap scenario

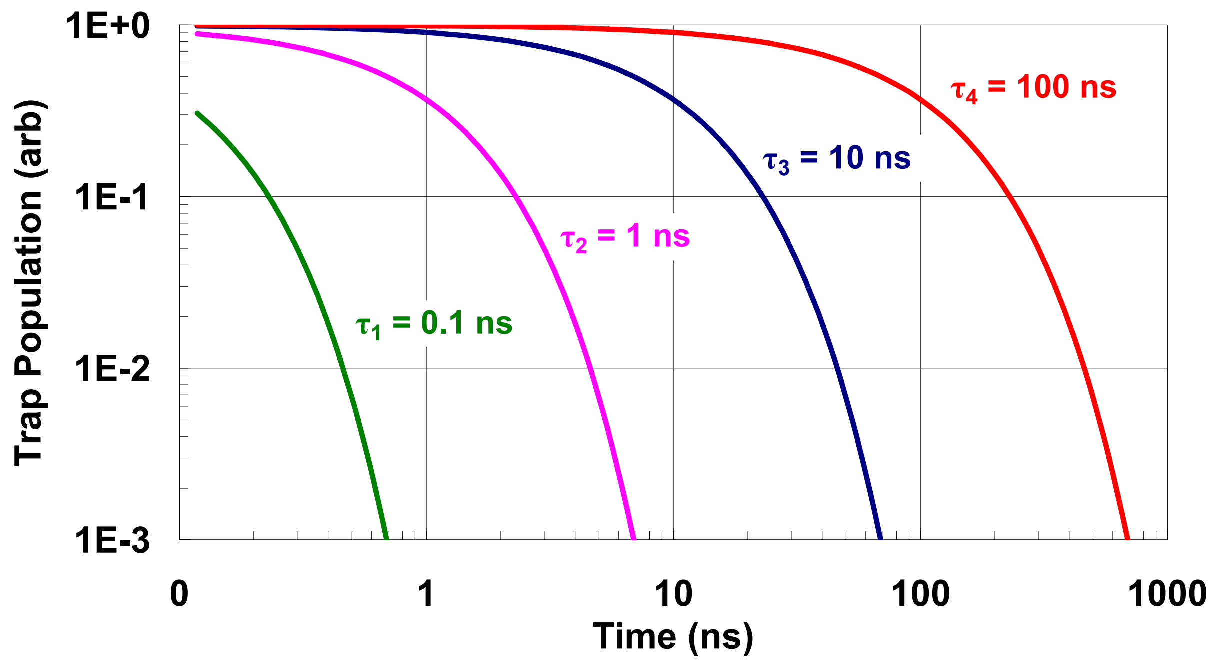

Survey of afterpulsing de-trapping times

- **Afterpulsing literature suggests multiple traps**
  - **De-trapping times identified over 4 orders of magnitude**
  - **But are these de-trapping times physically meaningful?**

Source	Temperature [K]	Hold-off time [μs]	Detrapping times [μs]				Technique
			τ_1	τ_2	τ_3	τ_4	
PLI/NASA	250	**0.14 – 0.46**	**0.07**				free-running
MIT/LL	250	**1.0 – 10**		**0.9**			double-pulse
Univ. Virginia	220 – 240	**0.02 – 50**	**0.15**	**1.0**	**5**	**45**	double-pulse
MagiQ	195 – 230	**1.25 – 100**		**0.5**	**6**	**100**	double-pulse
PLI/POLIMO	200 – 220	**4 – 1000**			**~15**	**~150**	DCR vs. $T_{h\text{-}o}$ scaling

Conclusions

- **Present DCR vs. DE performance**
  - **1.5 μm: ~10 kHz at 20% DE, T ~ 215 K, 25 μm dia.**
  - **1.06 μm: ~1 kHz at 30% DE, T ~ 235 K, 80 μm dia.**
- **DCR vs DE modeling provides good fit to experimental data**
  - **Illustrates trade-off between trap-assisted tunneling (TAT) and thermal generation**
  - **Activation energy studies confirm dominant mechanisms**
  - **Consensus forming around principal TAT defects**
- **Different approaches to afterpulse mitigation for higher repetition rate**
  - **Reduce initial carrier trapping → mostly a materials problem**
    - Increased operating temperature provides only modest impact on afterpulsing
  - **Reduce avalanche charge flow → operating conditions and design**
    - Lower overbias voltage (more quantitative analysis needed)
    - Reduced overbias duration using shorter gates or faster quenching
    - **Substantial opportunity for circuit design**